to appear in the *Astronomical Journal*

The Solar Neighborhood XXIV. Parallax Results from the CTIOPI 0.9-m Program: Stars with $\mu \geq 1\farcs0$ yr^{-1} (MOTION Sample) and Subdwarfs

Wei-Chun Jao[1], Todd J. Henry[1]

Department of Physics and Astronomy, Georgia State University, Atlanta, GA 30302

jao@chara.gsu.edu, thenry@chara.gsu.edu

John P. Subasavage[1]

Cerro Tololo Inter-American Observatory, La Serena, Chile

jsubasavage@ctio.noao.edu

Jennifer G. Winters[1], Adric R. Riedel[1]

Department of Physics and Astronomy, Georgia State University, Atlanta, GA 30302

winters@chara.gsu.edu, riedel@chara.gsu.edu

and

Philip A. Ianna[1]

Department of Astronomy, University of Virginia, Charlottesville, VA 22904-4325

philianna3@gmail.com

ABSTRACT

We present 41 trigonometric parallaxes of 37 stellar systems, most of which have proper motions greater than $1\farcs0$ yr^{-1}. These are the first trigonometric parallaxes for 24 systems. Overall, there are 15 red dwarf systems and 22 red subdwarf systems in the sample. Five of the systems are multiples with directly

[1]Visiting Astronomer, Cerro Tololo Inter-American Observatory. CTIO is operated by AURA, Inc. under contract to the National Science Foundation.

detected companions, and we have discovered perturbations caused by unseen companions in two additional cases, the dwarf LHS 501 and the subdwarf LHS 440. The latter system may eventually provide important dynamical mass points on the subdwarf mass-luminosity relation. Two additional stars of note are LHS 272, the third closest M-type subdwarf at a distance of only 13.6 pc, and LHS 2734AB, a high velocity subdwarf binary with $V_{tan} > 700$ km/sec, which likely exceeds the escape velocity of the Milky Way. We also report the first long term variability study of cool subdwarfs indicating that cool subdwarfs are less photometrically variable than their main sequence counterparts.

Subject headings: astrometry — solar neighborhood — stars: distances — stars: late-type — subdwarfs

1. Introduction

This is the sixth list of trigonometric parallaxes (hereafter, π_{trig}) from the Cerro Tololo Inter-American Observatory Parallax Investigation (CTIOPI) using data from the CTIO 0.9-m telescope. Previous papers reported parallaxes of stars from the MOTION sample (stellar systems with $\mu \geq 1\farcs0$ yr^{-1}, Jao et al. 2005), new members of the RECONS 10 pc sample (Henry et al. 2006), a young brown dwarf, (2MASSW J1207334−393254, Gizis et al. 2007), white dwarfs (Subasavage et al. 2009) and the SLOWMO sample (stellar systems with $0\farcs5 \leq \mu < 1\farcs0$ yr^{-1}, Riedel et al. 2010). In this paper, we target both MOTION stars and subdwarfs, presenting new π_{trig} for 24 stellar systems and improved π_{trig} for 13 additional systems. Such high proper motion stars are prime targets for parallax studies because they may be nearby — useful for luminosity and mass function studies, as well as being the closest representatives of their types — or they may be rare subdwarf members in the solar vicinity with high velocities. The overlap in these two samples makes it natural to combine the two types of objects in this paper. Twenty-nine of the systems are from the MOTION sample and are split into 14 red dwarf and 15 subdwarf systems. The remaining eight systems include seven additional subdwarfs and a red dwarf, LHS 3740 with a μ of nearly $1\farcs0$ yr^{-1}.

2. Observations and Data Reduction

2.1. Astrometry

The CTIO 0.9-m telescope has a 2048×2048 Tektronix CCD camera with $0\farcs401$ pixel^{-1} plate scale (Jao et al. 2003). For both astrometric and photometric observations, we use

the center quarter of the chip, yielding a 6′8 square field of view. Parallax frames are taken through one of four filters, $V_J(old)$, $V_J(new)$, R_{KC} or I_{KC}[1] (hereafter without the subscripts), so that either science or reference stars have maximum peak counts of ∼50,000 (saturation occurs at 65,535 counts) for better centroiding. The magnitudes of CTIOPI targets are $9 \leq VRI \leq 19$. Depending on the brightness of the science targets, reference stars, and sky conditions, exposure times vary from 20 to 1200 seconds. With few exceptions, observations are made within ±30 minutes of a science target's transit to minimize the corrections required for differential color refraction. Typically, three to 10 frames are taken in each night, depending primarily on the exposure time required. Bias and dome flat frames are taken nightly to enable routine calibration of the science images.

One "event" during the CTIOPI effort warrants special attention here. We have used two V filters, dubbed the "old" Tek#2 V filter ($\lambda_{central} = 5438$Å, $\Delta\lambda = 1026$Å) and "new" Tek#1 V filter ($\lambda_{central} = 5475$Å, $\Delta\lambda = 1000$Å), during the 11 years of observations because the "old" filter cracked in February 2005. The "new" V filter was used between 2005 and 2009. In July 2009, the old V filter was reinstated for use after confirming that the crack in the corner did not significantly affect astrometric residuals. We have found that as long as at least 1–2 years of data (depending on observing frequency) have been taken in both filters, the data can be combined to determine a reliable π_{trig} (Subasavage et al. 2009). In total, 10 of the 37 systems discussed in this paper were observed astrometrically in the V filter. Further details about the filters and their effects on the astrometry can be found in Subasavage et al. (2009) and Riedel et al. (2010).

The stellar paths traced by science stars on the sky are combinations of proper motions and parallactic shifts. Jao et al. (2005) and Henry et al. (2006) include extensive discussions of the data reduction processes used to separate these two movements. Briefly, we (1) use SExtractor (Bertin & Arnouts 1996) to measure centroids, (2) define a six-constant plate model to find plate constants (given in equation 4 of Jao et al. 2005), (3) assume that ensembles of reference stars have zero mean parallax and proper motion, (4) solve least-square equations for multi-epoch images (given in equation 5 of Jao et al. 2005), and (5) convert from relative parallax to absolute parallax by estimating the distance of the reference stars photometrically. The correction from relative to absolute parallax is accomplished using photometric distance estimates by comparing VRI colors to M_V for single, main sequence, stars in the RECONS 10 pc sample (Henry et al. 1997, 2004). For each reference star a distance is estimated, and the correction to absolute parallax is then computed using the weighted mean distance of the entire reference field. The error on the correction is determined

[1]The central wavelengths for the $V_J(old)$, $V_J(new)$, R_{KC} and I_{KC} filters are 5438, 5475, 6425, and 8075 Å, respectively. The old and new V filters are discussed in next paragraph.

using equation (6) in Jao et al. (2005).

2.2. Photometry

We have obtained VRI photometry of these targets at the CTIO 0.9-m telescope using the same instrumental setup used for the astrometry frames. Similar to those astrometry observations, bias and dome flat frames are taken nightly for basic image reduction. Most science stars were observed at $\sec z < 1.8$ or less (a few were observed between 1.8 and 2.0 airmasses because of extreme northern or southern declinations). Various exposure times were used to reach S/N > 100 for science stars in each of the VRI filters. Combinations of fields that provided 10 or more standard stars from Landolt (1992) and/or E-regions from Graham (1982) were observed several times each night to derive transformation equations and extinction curves. Further details of photometric data reduction, definition of transformation equations, errors, etc. can be found in Jao et al. (2005) and Winters et al. (2011).

2.3. Spectroscopy

Spectroscopic observations were made using the CTIO 1.5-m with the R-C spectrograph and Loral 1200×800 CCD camera. Grating #32 was used in first order with a tilt of 15.1°, and observations were made using a 2″ slit. The order-blocking filter OG570 was utilized to provide spectra covering the range of 6000Å to 9500Å with a resolution of 8.6Å. Bias frames, dome flats, and sky flats were taken at the beginning of each night for calibration.

At least two exposures were taken for each object to permit cosmic ray rejection, with additional exposures taken if stars were particularly faint. A 10 second Ne+He+Ar or Ne only arc lamp spectrum was recorded after each target to permit wavelength calibration. Several spectroscopic flux standard stars found in the $IRAF$ spectroscopy reduction packages were observed during each observing run, usually nightly. Reductions were carried out using $IRAF$ reduction packages — in particular *onedspec.dispcor* for wavelength calibrations and *onedspec.calibrate* for flux calibrations. We use the same set of spectral standard dwarfs discussed in Jao et al. (2008) to assign spectral types for dwarfs, and follow the same method discussed in that paper to assign spectral types for subdwarfs.

3. Astrometric Results

Parallax results for the 37 systems are given in Table 1. The single measurement accuracy for well-balanced reference fields with exposures at least a few minutes in duration is typically 2–8 mas. For weak reference fields (fewer than five reference stars, lopsided reference star configurations, or very faint reference stars), shorter exposure times, and close binaries with asymmetric point spread functions, the single measurement accuracy may be as high as 20 mas. Ultimately, the final absolute parallax errors for this sample of stars are 0.9–3.5 mas.

In Table 1, we present details about the astrometric observations (filters used, number of seasons observed, number of frames used in reductions, time coverage, span of time, and the number of reference stars) and results (relative parallaxes, parallax corrections, absolute parallaxes, proper motions, position angles of the proper motions, and the derived tangential velocities based on relative proper motions given in column 12). Twenty-four of the 37 systems discussed here had no previous π_{trig}. These systems are listed in the top portion of the table. The remaining 13 systems shown in the bottom of Table 1 have π_{trig} previously reported in van Altena et al. (1995) (hereafter YPC), Jao et al. (2005), Smart et al. (2007), or Bartlett et al. (2009). Figure 1 shows the HR diagram of these targets and we will discuss individual systems later in Section 6. The astrometric, photometric, and spectroscopic results presented here supersede those in Jao et al. (2005) because additional data and improved reduction techniques have been used, as discussed in detail in Subasavage et al. (2009).

4. VRI Photometry

New VRI photometry for the 37 systems is given in Table 2, as well as the near-infrared photometry (J, H, and K_s bands) from the Two Micron All Sky Survey (Skrutskie et al. 2006). Names are given in the first two columns, followed by the optical VRI photometry in columns 3–5, the number of nights (column 6) on which VRI observations were taken. The information used for the photometric variability (see Section 5) is listed in columns 7–9. The JHK_s photometry is given in columns 10–12. All of the systems have at least two nights of VRI photometry data. The mean errors of VRI photometry are usually $\leq$ 0.03 mag. However, stars that are faint at V sometimes have larger errors, e.g. the faintest star, SIPS 1529−2907 with V=19.38, has the largest S/N error of 0.12 mag. The remainder of these parallax targets have S/N error less than 0.07 mag at V. See Winters et al. (2011) for a detailed discussion of our VRI photometry program errors.

The V photometry given here represents combined values from the two different V filters

discussed in Section 2.1. To check the consistency of photometry from these two filters, we selected ten photometric standard stars observed between 2001 and 2009 on a total of 45 photometric nights, including 20 nights of photometry in the "old" V filter and 25 nights of photometry in the "new" V filter. The ten stars selected were SA98-670 (V =11.93), SA98-650 (V=12.27), SA98-676 (V=13.07), SA98-671 (V=13.39), SA98-675 (V=13.40), and SA98-682 (V=13.75) from Landolt (1992), E2-o (V=14.09), E2-t (V=14.60), and E2-I (V=15.17) from Graham (1982) and GJ 406 (V=13.57) from Kilkenny et al. (1998). The $V-I$ colors of these standard stars are between 0.20 and 4.12.

The differences between the measured V magnitudes for the standards relative to their quoted magnitudes in the original photometric standards papers are plotted in Figure 2. It is clear that the two filters yield effectively identical V band photometry for these ten standard stars. The mean differences are 0.006 and 0.007 mag from the "old" and "new" V filters, respectively, which is much less than our quoted 0.03 mag error. Hence, we conclude that the V band photometry from the two filters can be combined.

5. Variability Studies

5.1. Analysis

In addition to the VRI photometry, we take advantage of our long-term observations of these fields (up to 10 years) in the parallax filter (column 7 in Table 2) to analyze the photometric variability (column 8 in Table 2) of these parallax targets. The total number of nights used for the variability study for each star is given in column 9 in Table 2.

Here we examine 130 red dwarfs for evidence of variability, as measured by the standard deviations, σ_{mag}, of magnitudes derived relative to reference stars in the fields. Combining the 41 stars in this paper with stars in Henry et al. (2006) and Riedel et al. (2010), two previous papers with similar data streams, yields a total of 135 stars. We exclude five stars from the study, as follows. GJ 1207, with $\sigma_{mag} = 0.263$ (Henry et al. 2006), was observed during an obvious flare in a single series of observations. LP 771−095BC, with $\sigma_{mag} = 0.043$ (Henry et al. 2006), exhibited a sudden ∼0.3 magnitude drop in brightness at V on UT 1999 August 21, but LP 771−095A, the primary star, and none of the reference stars showed this event (one possible cause is an eclipse). LHS 193B, with $\sigma_{mag} = 0.049$ (this work), is a white dwarf that was underexposed in all frames because the primary, LHS 193A, was the star targeted for parallax. Similarly, LHS 2734A was the parallax target, so LHS 2734B with $\sigma_{mag} = 0.020$ (this work) was systematically underexposed and has been omitted from the analysis. Finally, as discussed below in §5.2, the photometry for LHS 272 with $\sigma_{mag} = 0.015$

(this work) was corrupted by a background galaxy.

To evaluate variability, we first extracted the instrumental magnitudes using SExtractor with a fixed 6″ diameter aperture. Because most parallax frames were taken on nights when photometric standard stars were not observed, we do not convert instrumental magnitudes to apparent magnitudes; we instead compare the relative fluxes of the target stars to the reference stars used to set the astrometric grid. We follow the methodology discussed in Honeycutt (1992) to handle an inhomogeneous set of exposures. The basic equation of condition used to evaluate inhomogeneous sets of exposures is

$$m_i^j = m0_i + \delta m^j, \tag{1}$$

where m_i^j is the instrumental magnitude of star i on image j (magnitude output from SExtractor), $m0_i$ is the mean instrumental magnitude of star i, and δm^j is the magnitude offset for image j. In other words, δm^j takes into account the differences caused by sky conditions, extinction, and exposure times for each frame in the series. We then utilize a Gauss-fit program (Jefferys, Fitzpatrick & McArthur 1987) to perform least-square calculations to minimize the deviations between the two sides of this equation of condition, as described in more detail in Honeycutt (1992).

After obtaining δm^j, the "corrected" instrumental magnitude (mc_i^j) is

$$mc_i^j = m_i^j - \delta m^j. \tag{2}$$

We then calculate the σ_{mag} values of the corrected instrumental magnitudes, mc_i^j, in a given filter for all science and parallax reference stars in that field. An example output is shown in the top of Figure 3. Naturally, the standard deviation is a function of magnitude, where fainter stars have larger standard deviations. In column 8 of Table 2, we list the standard deviations in magnitudes for the science stars. A high standard deviation value for a science or reference star can be caused by (1) a flare occurring during a series of observations on one night, (2) long term variability, (3) contaminated photometry from a nearby source, (4) high sky background caused by moon illumination or a twilight sky[2], or (5) faint reference stars in the field. Only the first two causes are indicative of true variability.

If a reference star's magnitude appears to have a high standard deviation, as illustrated

[2]In order to get high parallax factors during astrometric measurements, we sometimes take frames during evening and morning nautical twilight when the center of the Sun is about 11 degrees below the horizon, with consequently high sky background.

with an open box shown in the top panel of Figure 3, we remove this outlier and perform another round of least-square calculations to obtain the δm^j values for the frames and the final mc_i^j and derived σ_{mag} values. Such outliers can be caused by any of the five reasons listed above. Usually, after the second round of calculations to get mc_i^j, we determine the final magnitudes for the science star for each frame, which represents its variability around its mean magnitude, as shown in the bottom of Figure 3.

We have carried out three specific tests to support the variability results, including analyses of (1) the two V filters used, (2) reference star selection, and (3) the target star brightness ranking relative to the reference stars.

Two V Filters: To check that slight differences between the two V filters ("old" and "new") do not cause significant extra variability for those parallax stars observed using both filters, we have evaluated the photometric time series of three white dwarfs, LHS 145, GJ 440 and GJ 781.3, observed during CTIOPI (Subasavage et al. 2009). These three stars have rich datasets taken using both filters and are known to be non-pulsating white dwarfs, which ensures extremely low levels of intrinsic variability. The results given in Table 3 show that in both filters, our "observational floor" for detecting variability is ∼0.008 mag (discussed further in §5.2). Thus, the use of different V filters may introduce small additional uncertainities. However, the "observational floor" in V stays below 0.010 mag.

Reference Star Selection: To investigate whether or not the reference stars' brightnesses affect δm^j, and consequently our measurements of variability, we have selected the reference star rich field of LHS 3045 for a series of tests in which we keep the total number of reference stars constant. Figure 4 shows results using four different sets of reference stars. Setup 1 is the one used for the parallax reduction reported in Table 1 and the variability result given in Table 2. Setup 2 includes three stars that differ from those in Setup 1 so that the mean magnitude of the Setup 2 reference stars is brighter than for Setup 1. Setup 3 includes a set of faint reference stars that could be selected in this field (but wouldn't, given much more suitable reference stars). Setup 4 also includes reference stars that are all fainter than LHS 3045, but which are generally brighter than in the case of Setup 3.

Setups 1 and 2 have identical standard deviations for all stars in common. Setup 2 was not chosen for the parallax work because some stars are on the edge of the CCD chip, where their PSFs are slightly distorted and degrade the astrometric results. Predictably, Setup 3 yields the highest standard deviations among the tests because all of the reference stars are fainter than mag 19.8. In practice, these stars cannot be selected for astrometric work because they are too faint to determine reliable centroids if the target star is kept unsaturated. As discussed in §2.1, to derive good centroids for astrometric measurements, we expose long enough to let either parallax or reference stars reach peak counts of ∼50,000

for centroiding, which consequently provides a high S/N for all stars used in the astrometric reduction. In fact, because the target/reference star configuration used in Setup 3 will not provide a reliable parallax, we would drop this target from the parallax program. We did not select Setup 4 because suitable brighter stars were available for both astrometric and photometric work. The σ_{mag} values from Setup 4 are 0.001 mag higher than for Setups 1 and 2 because of four stars of mag 19.7 or fainter. Nonetheless, the σ_{mag} value for the target star remains less than 0.010 mag and is only 0.001 mag higher than for Setups 1 and 2. We therefore conclude that all realistic reference star configurations yield variability measurements consistent at the 0.001 mag level.

Target Star Brightness: To better understand how variability measurements change with the brightness ranking of the target star, in Figure 5 we plot the σ_{mag} values vs. magnitude for the 130 sample stars, and show the brightness ranking of the target stars in the right panel. A science star with a brightness ranking of 85% means that 85% of reference stars in that field are fainter than the science star. A science star with brightness ranking of almost 100% has a field similar to Setup 4 in Figure 4. The mean brightness ranking of all 130 stars is ∼85%, marked as a vertical dashed line. The right panel of Figure 5 shows that there is no clear relation between a science target's brightness ranking and its variability for most stars, which are found in the 50–100% region.

Overall, we conclude that none of the three tests indicates any systematic effects on the variabilities measured for the target stars.

5.2. Variability Results

Figure 6 shows stellar variability, measured using σ_{mag}, as a function of color for the 130 dwarfs and subdwarfs included in this study, separated into panels that include all stars and split into subsets for stars observed in the V, R, and I filters. Points with Xs are the five stars omitted from the statistical study, for reasons given in §5.1. For the sample of 108 dwarfs (open circles in Figure 6), the mean variabilities at V, R, and I, are 0.013 (51 stars), 0.013 (39 stars), and 0.008 (18 stars) mag, respectively. These results indicate that as a group, red dwarfs are more variable in the V and R bands than in the I band. We also perform a Kolmogorov-Smirnov test for 51 stars at V band and 18 stars at I band. The result shows a probability of 99.87% that distributions of these two bands are statistically different.

For the sample of 22 cool subdwarfs, the average variabilities are 0.007 at V (3 stars), 0.008 at R (13 stars), and 0.007 at I (6 stars) mag, which are lower than for dwarfs at V and

R. A Kolmogorov-Smirnov test for the R band sample, in which we have the largest number of subdwarfs, indicates a probability of 100% that the dwarf and subdwarf cumulative distributions are different, where the greatest absolute difference between the two distributions is equal to 0.74, highly indicative of different samples. Thus, it appears that the variability in subdwarfs is lower than that of dwarfs, at least in the R band, implying that their atmospheres are less active. More subdwarfs need to be observed in the V band to confirm our suspicion of less activity than for subdwarfs than for dwarfs at V, although the data do point in that direction. We also note that subdwarf variability is similar in all three filters, rather than increasing at shorter wavelengths, which is the case for dwarfs. This may be indicative of quiet atmospheres in the subdwarfs, for which we have reached our "observational floor" (about 0.008 mag) in our ability to measure variability in the current datasets, which suspiciously also matches the value for the least variable I filter measurements for dwarfs. Although this comparison is based on relatively small samples, it is the first time the long-term variability of cool subdwarfs has been investigated[3].

Overall, most subdwarfs' variability is less than 0.01 mag, with two notable exceptions, both of which have been excluded in the statistical evaluations of the subdwarf sample above:

LHS 272 This star is relatively bright ($V = 13.16$), yet has the largest $\sigma_V = 0.015$ of the 11 stars measured in that field. For comparison, a relatively faint ($V = 14.17$) reference star has $\sigma_V = 0.007$. However, LHS 272 was observed on the wing of a bright background galaxy $\sim$17″ distant at a position angle of 217° in 2001. In our frames, LHS 272 has moved quickly away at $\mu = 1.439$ yr^{-1} at 279.2°, but the galaxy may corrupt the variability measurements for those images taken during the first few epochs of observations, causing an erroneously high variability measurement.

LHS 2734B This is the fainter star of a pair of science targets in the field; the primary, LHS 2734A was targeted for parallax so the B component was systematically underexposed, resulting in a high variability measurement due to poor S/N, with $\sigma_I = 0.020$ mag. This is also the faintest star observed among all 130 systems, with $I = 16.79$.

So far, we have only observed a few dozen subdwarfs over these long time periods, and with limited numbers of reference stars. At present, we are comparing subdwarfs observed at R with $V - I < 2.4$ to dwarfs observed at R with $V - I > 2.4$, as shown in Figure 6. In order to make a systematic comparison of dwarfs and subdwarfs of similar color, we need long-term photometric monitoring campaigns that cover large swaths of sky, such as the Hungarian-made Automated Telescope Network (HATNet) or the All Sky Automated

[3]We note that there are numerous publications concerning the variability of hot "subdwarfs" because of their pulsations, but they are fundamentally different from the "cool subdwarfs" discussed here.

Survey (ASAS). For example, Hartman et al. (2009) reported variability for 27,560 K and M dwarfs using HATNet data, but this rich dataset has not yet been applied to subdwarfs. The catch is that these surveys typically reach $\sigma_{mag} \sim 0.01$ mag at $I \sim 11$, a magnitude limit too bright to reach many cool subdwarfs. To reach large numbers of faint, cool, subdwarfs, we will need the next generation of survey projects like the Large Synoptic Survey Telescope (LSST), the Panoramic Survey Telescope and Rapid Response System (Pan-STARRS), and the SkyMapper project.

6. Notes on Individual Systems

G 266-089A and B These stars comprise a resolved binary system also known as LHS 111 (A) and LHS 110 (B). The separation is $9\farcs02$ at position angle 321.1° (Jao et al. 2003), a separation that allows individual parallaxes to be determined for the two components. The weighted mean of the two measurements is $\pi_{trig} = 33.75 \pm 1.20$ mas. At a distance of 29.6 pc, this measured separation corresponds to a projected separation of ∼270 AU, so we do not expect to see any orbital motion during the ∼5 years of astrometric observations. Bidelman (1985) reported spectral types of M3.5V and M4.0V for A and B, respectively. We report a joint spectrum for the combined system because both stars fell in the slit during acquisition, and the individual spectra were not sufficiently separated on the chip for reliable individual reductions. The spectrum indicates dwarf features, but both stars fall below the main sequence, as shown in Figure 1. We therefore note this system as M4.0J[VI] (J = joint) until we obtain separate spectra.

LSR 0627+0616 A single image from the first epoch extends the astrometric coverage from 2.97 years to 6.07 years. The parallax error drops from 1.33 to 1.25 mas, while the proper motion error drops from 1.2 to 0.9 mas yr^{-1}.

LHS 272 With $\pi_{trig} = 73.95 \pm 1.18$ mas (13.53 ± 0.22 pc), this is the third closest M-type subdwarf found to date. Only Kapteyn's star with $\pi_{trig} = 255.27 \pm 0.86$ mas (3.92 ± 0.02 pc, weighted mean parallax from YPC and Hipparcos) and μ Cas B with $\pi_{trig} = 132.57$ ± 0.57 mas (7.54 ± 0.04 pc, weighted mean parallax from YPC and Hipparcos) are closer. The fourth closest known M subdwarf, LHS 20, is at 62.40±3.30 mas or 16.07 ± 0.85 pc (YPC). We do not detect a perturbation by an unseen companion of LHS 272 over ∼4 years of data, nor do we see any companions via optical speckle observations (Jao et al. 2009).

LHS 327 Augensen & Buscombe (1978) commented that this star had a total space velocity of 582 km sec^{-1} and would escape from the Galaxy. However, Ryan & Norris (1991) reported $V_{rad} = 80$ km/sec, from which we derive a total space velocity of 430 km sec^{-1}. This

star may therefore be marginally bound to the Galaxy because the Galactic escape velocity is estimated to be between 450 and 650 km/sec (Leonard & Tremaine 1990).

LHS 347 This is an early K type star and is below the main sequence with a relatively large error bar, as shown in Figure 1. However, its spectrum is almost identical to a K2.0V dwarf. Because of its high V_{tan} = 331.3 km sec^{-1}, and low luminosity, we assign it a type K2.0[VI], representing its uncertain assignment as a subdwarf.

LHS 2734AB This is a binary with separation 68.″8 at position angle 162.3°. We find different relative trigonometric parallaxes for LHS 2734 A (2.79 mas) and B (−1.70 mas). The system is too far away for us to measure a meaningful parallax, given that $\pi^A_{rel}/\sigma_{\pi^A_{rel}} \sim 2.3$ and $\pi^A_{rel}/\pi^A_{corr} \sim 2.4$. The secondary is 2.2 mag fainter than the primary at I, the filter used for astrometric measurements. Thus, B is underexposed in the images, so we have adopted A's absolute parallax for B in Table 1. Using our new π_{trig}, we find that the system has $V_{tan} > 700$ km/sec, although this value is highly uncertain. Nevertheless, V_{tan} is certainly large, and this system may be able to escape the Galaxy.

LHS 3045 This has astrometric residuals indicative of a possible perturbation in the RA axis, but not in DEC axis. The perturbation is not seen in reference star residuals, lending credence to its veracity. We will continue to observe the star to confirm or refute the trend. Bidelman (1985) reported a spectral type of K5V, but its location in Figure 1 shows that it is clearly in the subdwarf region, and a [VI] spectral type is given in Table 2. A spectroscopic observation is needed to confirm its luminosity class.

LHS 3732 Ibata & Irwin (1997) report this star to be a subdwarf and its position in Figure 1 ($(V-K) = 3.11$) indicates that it a subdwarf of early K type. Our measured proper motion of 0.″959/yr and parallax of 8.34 ± 1.58 mas yield V_{tan} ∼550 km/sec. Augensen & Buscombe (1978) reported V_{rad} = 120 km/sec, which results in $(U,V,W)^4 \approx$ (−48,−522,−141) km sec^{-1}. The total space velocity is ∼543 km/sec, indicating that the star may not be bound to the Galaxy. We note that nearly all of the velocity contribution is a result of the V_{tan} measurement, which is based on a large, and relatively poorly known, distance.

LHS 318 Smart et al. (2007) reported π_{trig} = 24.8±6.0 mas. Our parallax of 18.76±2.32 mas is consistent with their measurement, with a smaller error by a factor of 2.6.

LHS 326 Smart et al. (2007) reported π_{trig} = 11.7±4.3 mas. Our parallax of 20.39±1.94 mas is marginally consistent with their measurement, with a smaller error by a factor of 2.2.

---

[4]This is a velocity relative to the Local Standard of Rest (LSR), where the solar motion is ($U_\odot$, $V_\odot$, $W_\odot$)=(+11.1, +12.24, +7.25) km sec^{-1} with respect to the LSR (Schönrich et al. 2010).

LHS 440 As shown in Figure 7, this star shows a convincing perturbation in the residuals on the DEC axis that is possibly confirmed in the RA axis. The period is longer than 10 years, so the star will remain on CTIOPI because it is subdwarf of type M1.0VI (Jao et al. 2008), making it a rare example of a nearby subdwarf binary that may eventually yield important dynamical masses.

LHS 499 Images taken during the first season used the old V filter, while the rest of three seasons were observed using new V. Our $\pi_{trig} = 56.93 \pm 2.12$ mas uses data from both filters and is consistent with the YPC value of 63.0 ± 11.7 mas with a smaller error by a factor of 5.5.

LHS 501 and LHS 500 This is a wide common proper motion binary with separation $107\farcs1$ at position angle 185.2° (Jao et al. 2003). LHS 501, the primary star A, shows a perturbation on both axes, as shown in Figure 7. We do not yet have sufficient data to derive an orbit, but the system will remain on CTIOPI. The perturbation is likely the cause of the discrepant parallaxes and proper motions determined for A and B, where the values for the B component are more reliable. Preliminary high resolution imaging using the Gemini-North adaptive optics system (ALTAIR) and Near InfraRed Imager (NIRI) in 2009 has resolved the tertiary near LHS 501. Details about these AO results will be discussed in a future paper.

LHS 521 This star shows a possible perturbation in DEC that does not appear in the series for any reference star. However, more observations are needed to confirm the perturbation.

GJ 1277 Our relative parallax measurement of 96.31 ± 0.95 mas is consistent with the relative parallax measurement of 94 ± 1.0 mas reported by Bartlett et al. (2009), who did not provide an absolute parallax.

7. Summary

We present 41 new and revised trigonometric parallaxes of 37 systems, of which 15 are red dwarfs and 22 are subdwarfs. By combining the results of this paper, Jao et al. (2005), Costa et al. (2005), and Costa et al. (2006) (the latter two papers from our CTIO 1.5-m parallax program), we have now determined parallaxes for 32 subdwarf systems. This comprises the largest set of cool subdwarf parallaxes since Monet et al. (1992)'s effort that included 21 cool subdwarf systems. Our continuing efforts will further increase the number of nearby subdwarfs with accurate parallaxes (errors less than 10%), and will allow us to better characterize the population of cool subdwarfs in the solar neighborhood.

Unlike dwarfs, subdwarfs show very different spectroscopic "flavors" depending on their metallicities and gravities (Jao et al. 2008). This is evident in Figure 1, where the spread in M_{Ks} is greater than three magnitudes for some $(V - K_s)$ colors. Thus, building useful combinations of $VRIJHK_s$ photometry to estimate distances to subdwarfs is far more difficult than for dwarfs, which is relatively straightforward (Henry et al. 2004). In fact, if one wrongly applies relations for main-sequence dwarfs or incorrect subdwarf "flavors" to a specific subdwarf, it will be estimated to be either further away or much closer that it truly is. By measuring more trigonometric parallaxes and accurate photometry for cool subdwarfs, we can develop better distance estimating techniques and perhaps reveal more nearby subdwarfs like LHS 272.

In the process of investigating the present sample of high proper motion stars and subdwarfs, we have detected a rare close subdwarf binary (LHS 440) as well as a dwarf binary (LHS 501) via astrometric perturbations. The only cool subdwarf with an accurate mass measurement is μ Cas B (0.17 $M_\odot$, McCarthy et al. 1993). Our continued astrometric efforts coupled with future radial velocity observations will yield essential mass measurements for low-mass subdwarfs, and thus provide important dynamical mass points on the subdwarf empirical mass-luminosity relation.

Finally, we have used our long term parallax observations to compare the photometric variability of cool dwarfs and subdwarfs. Subdwarfs appear to be less variable than dwarfs in the R band, where we have the most data points, and possibly less variable than dwarfs in the V band. However, our variability techniques should be applied to much larger subdwarf samples to confirm these intriguing results.

8. Acknowledgments

The astrometric observations reported here began as part of the NOAO Surveys Program in 1999 and continued on the CTIO 0.9-m via the SMARTS Consortium starting in 2003. We gratefully acknowledge support from the National Science Foundation (grants AST 05-07711 and AST 09-08402), NASA's Space Interferometry Mission, and Georgia State University, which together have made this long-term effort possible.

We thank the referee to provide comments to improve this paper. We thank Po-Yung Chen for his efforts on statistics. We also thank the members of the SMARTS Consortium, who enable the operations of the small telescopes at CTIO, as well as the supporting observers support at CTIO, specifically Edgardo Cosgrove, Arturo Gómez, Alberto Miranda, and Joselino Vásquez. This research has made use of the SIMBAD database, operated at CDS,

Strasbourg, France. This work also has used data products from the Two Micron All Sky Survey, which is a joint project of the University of Massachusetts and the Infrared Processing and Analysis Center at California Institute of Technology funded by NASA and NSF.

REFERENCES

Augensen, H. J., & Buscombe, W. 1978, Ap&SS, 59, 35

Bartlett, J. L., Ianna, P. A., & Begam, M. C. 2009, PASP, 121, 365

Bertin, E. & Arnouts, S. 1996, A&AS, 117, 393

Bidelman, W. P. 1985, ApJS, 59, 197

Costa, E., Méndez, R. A., Jao, W.-C., Henry, T. J., Subasavage, J. P., Brown, M. A., Ianna, P. A., & Bartlett, J. 2005, AJ, 130, 337

Costa, E., Méndez, R. A., Jao, W.-C., Henry, T. J., Subasavage, J. P., & Ianna, P. A. 2006, AJ, 132, 1234

Dieterich, D. 2010, in preparation

The *Hipparcos* and Tycho Catalogues, 1997, ESA SP-1200 (Noordwijk: ESA)

Gizis, J. E. 1997, AJ, 113, 806

Gizis, J. E., Jao, W.-C., Subasavage, J. P., & Henry, T. J. 2007, ApJ, 669, L45

Graham, J. A. 1982, PASP, 94, 244

Hartman, J. D., Bakos, G. Á., Noyes, R. W., Sipöcz, B., Kovács, G., Mazeh, T., Shporer, A., & Pál, A. 2009, arXiv:0907.2924

Hawley, S. L., Gizis, J. E., & Reid, I. N. 1996, AJ, 112, 2799

Henry, T. J., Ianna, P. A., Kirkpatrick, J. D., & Jahreiß, H. 1997, AJ, 114, 388

Henry, T. J., Walkowicz, L. M., Barto, T. C., & Golimowski, D. A. 2002, AJ, 123, 2002

Henry, T. J., Subasavage, J. P., Brown, M. A., Beaulieu, T. D., Jao, W., & Hambly, N. C. 2004, AJ, 128, 2460

Henry, T. J., Jao, W.-C., Subasavage, J. P., Beaulieu, T. D., Ianna, P. A., Costa, E., & Méndez, R. A. 2006, AJ, 132, 2360

Honeycutt, R. K. 1992, PASP, 104, 435

Ibata, R. A., & Irwin, M. J. 1997, AJ, 113, 1865

Jao, W.-C., Henry, T. J., Subasavage, J. P., Bean, J. L., Costa, E., Ianna, P. A., & Méndez, R. A. 2003, AJ, 125, 332

Jao, W.-C., Henry, T. J., Subasavage, J. P., Brown, M. A., Ianna, P. A., Bartlett, J. L., Costa, E., & Méndez, R. A. 2005, AJ, 129, 1954

Jao, W.-C., Henry, T. J., Beaulieu, T. D., & Subasavage, J. P. 2008, AJ, 136, 840

Jao, W.-C., Mason, B. D., Hartkopf, W. I., Henry, T. J., & Ramos, S. N. 2009, AJ, 137, 3800

Jefferys, W. H., Fitzpatrick, M. J., & McArthur, B. E. 1987, Celestial Mechanics, 41, 39

Kilkenny, D., van Wyk, F., Roberts, G., Marang, F., & Cooper, D. 1998, MNRAS, 294, 93

Landolt, A. U. 1992, AJ, 104, 340

Leonard, P. J. T., & Tremaine, S. 1990, ApJ, 353, 486

Lépine, S., Rich, R. M., & Shara, M. M. 2003, AJ, 125, 1598

McCarthy, D., Jr., et al. 1993, AJ, 105, 652

Monet, D. G., Dahn, C. C., Vrba, F. J., Harris, H. C., Pier, J. R., Luginbuhl, C. B., & Ables, H. D. 1992, AJ, 103, 638

Riedel et al, 2010, accepted to AJ

Smart, R. L., Lattanzi, M. G., Jahreiß, H., Bucciarelli, B., & Massone, G. 2007, A&A, 464, 787

Ryan, S. G., & Norris, J. E. 1991, AJ, 101, 1835

Schönrich, R., Binney, J., & Dehnen, W. 2010, MNRAS, 403, 1829

Skrutskie, M. F., et al. 2006, AJ, 131, 1163

Subasavage, J. P., Jao, W.-C., Henry, T. J., Bergeron, P., Dufour, P., Ianna, P. A., Costa, E., & Méndez, R. A. 2009, AJ, 137, 4547

van Altena, W. F., Lee, J. T., & Hoffleit, D. 1995, The General Catalogue of Trigonometric Stellar Parallaxes (4th ed.; New Haven: Yale Univ. Obs.)

Winters, J. G., Henry, T. J., Jao, W.-C., Subasavage, J. P., Finch, C. T., & Hambly, N. C. 2011, AJ, 141, 21

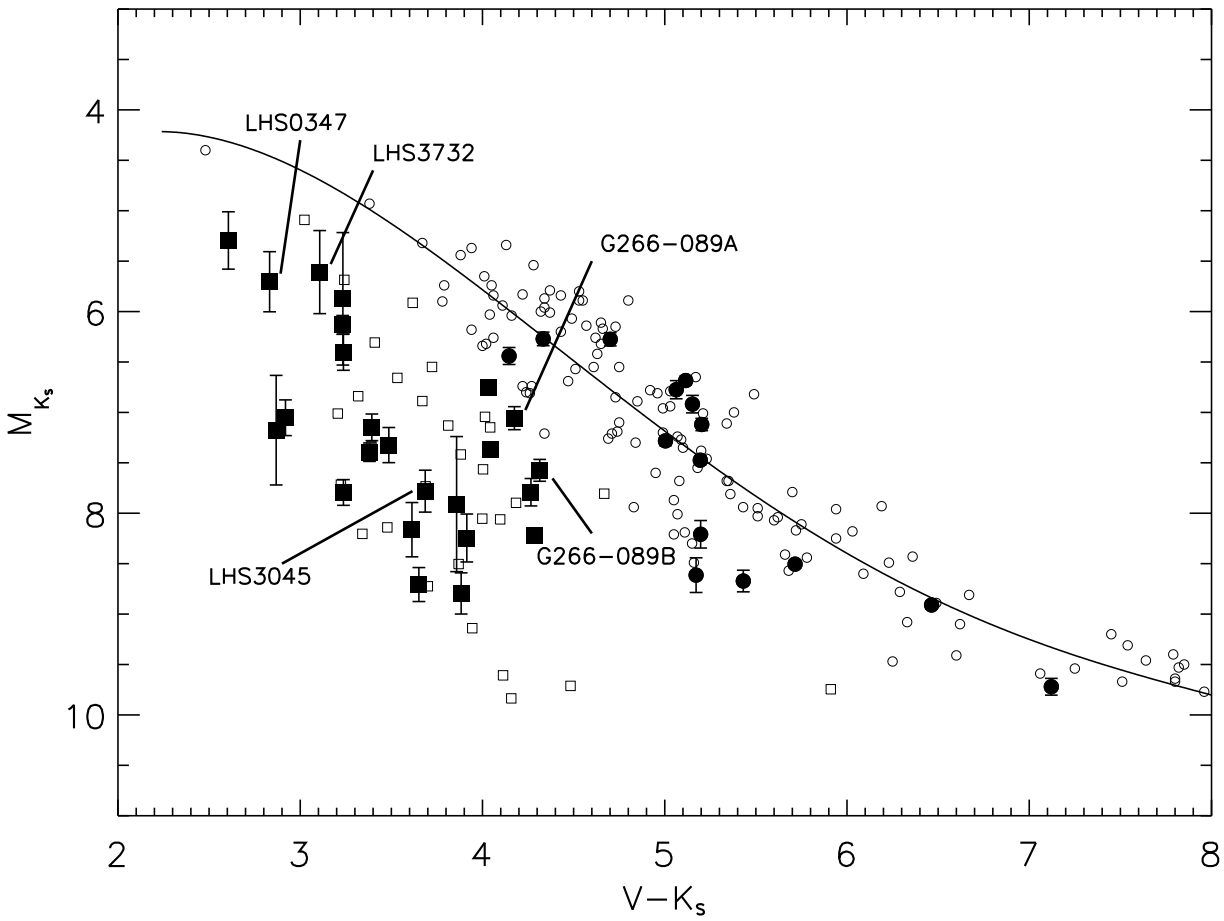

Fig. 1.— The HR diagram, using M_{K_s} vs. $V-K_s$, is shown for 41 stars in the 37 systems outlined in Tables 1 and 2. Filled boxes and circles indicate subdwarfs and dwarfs, respectively. Open boxes represent 32 subdwarfs (LHS stars with $\mu > 1\farcs0$ yr^{-1}) from Gizis (1997). Open circles represent RECONS sample members (*www.recons.org*) and some very late M dwarfs discussed in Henry et al. (2004), with an empirical fit tracing the main sequence stars. Some stars discussed in Section 6 regarding their locations on the HR are labeled here.

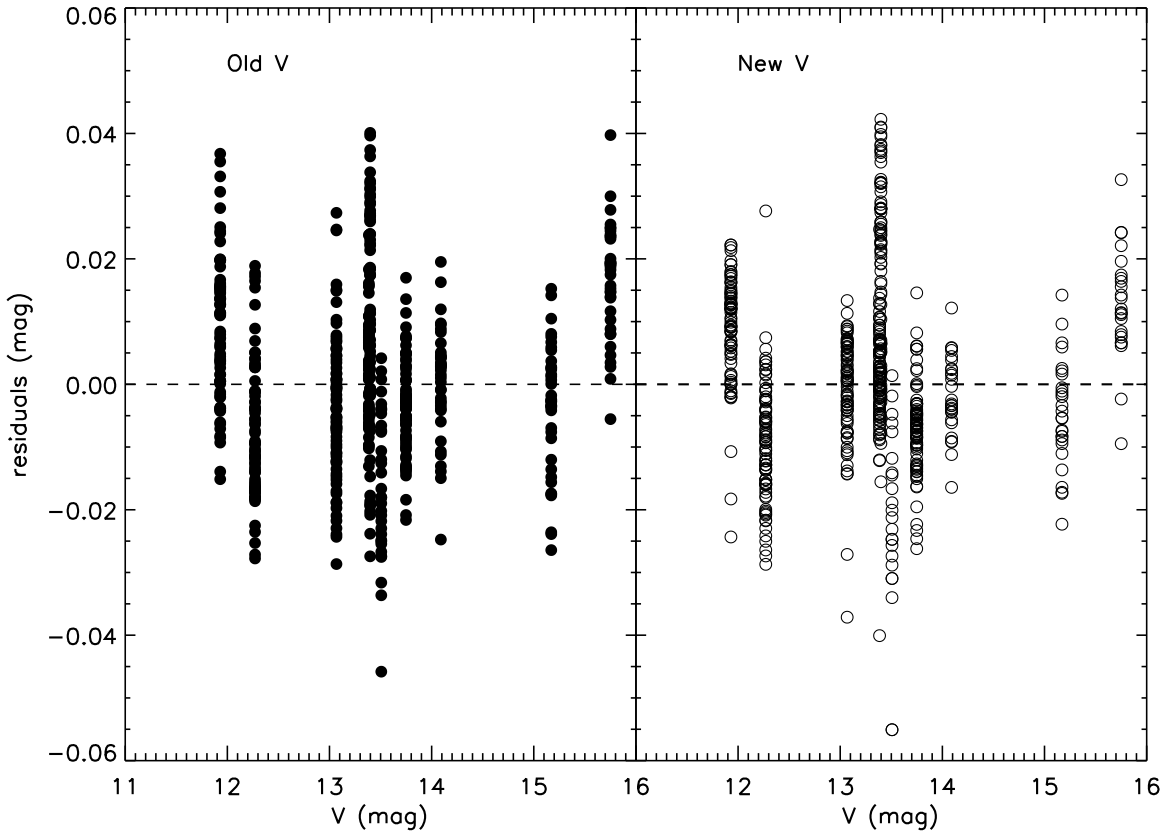

Fig. 2.— Differences between reported magnitudes and our derived magnitudes are shown for ten photometric standard stars observed between 2001 and 2009 through two V filters. Left (solid circles) and right (open circles) panels indicate stars observed with "old" and "new" V filters, respectively. The dashed line indicates identical magnitudes derived from our measurements when compared to magnitudes in the photometric standard papers. Note that SA98-671 (V=13.39) and SA98-675 (V=13.40) overlap in this figure because of the scale of these plots. There are no obvious systematic differences seen for the two filters.

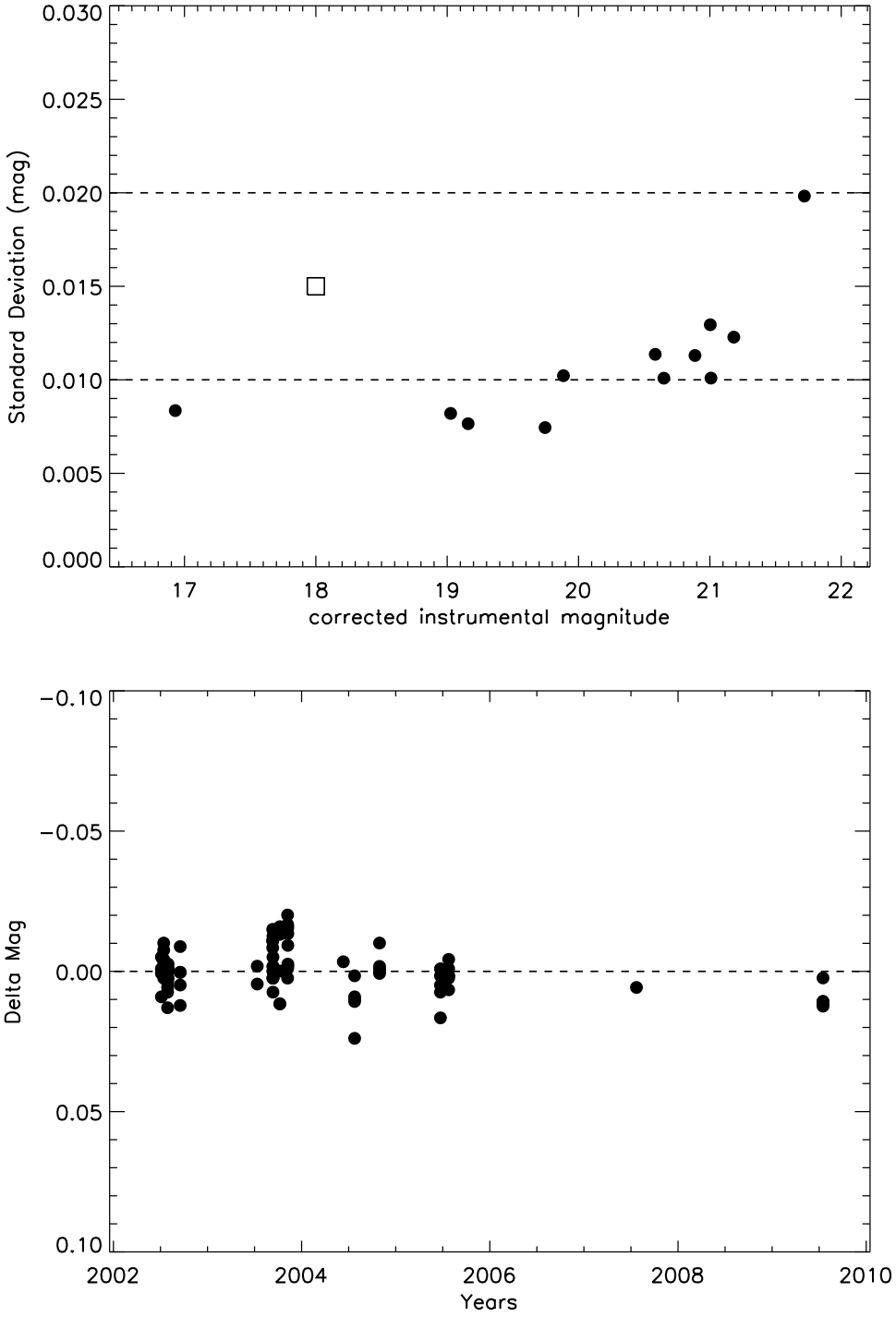

Fig. 3.— A variability study of LHS 518. Top: This plot shows corrected instrumental magnitudes, (mc_i^j), in the R band and standard deviations, σ_{mag}, of 12 stars in the field of LHS 518. The brightest point at the far left represents LHS 518. An open box simulates an outlier star with unusually high standard deviation that would be discarded before deriving the final σ_{mag} value of LHS 518. Bottom: The light curve of LHS 518 is shown around its mean magnitude. Its standard deviation (0.008 mag) is calculated using all of the images shown from 18 nights of observations.

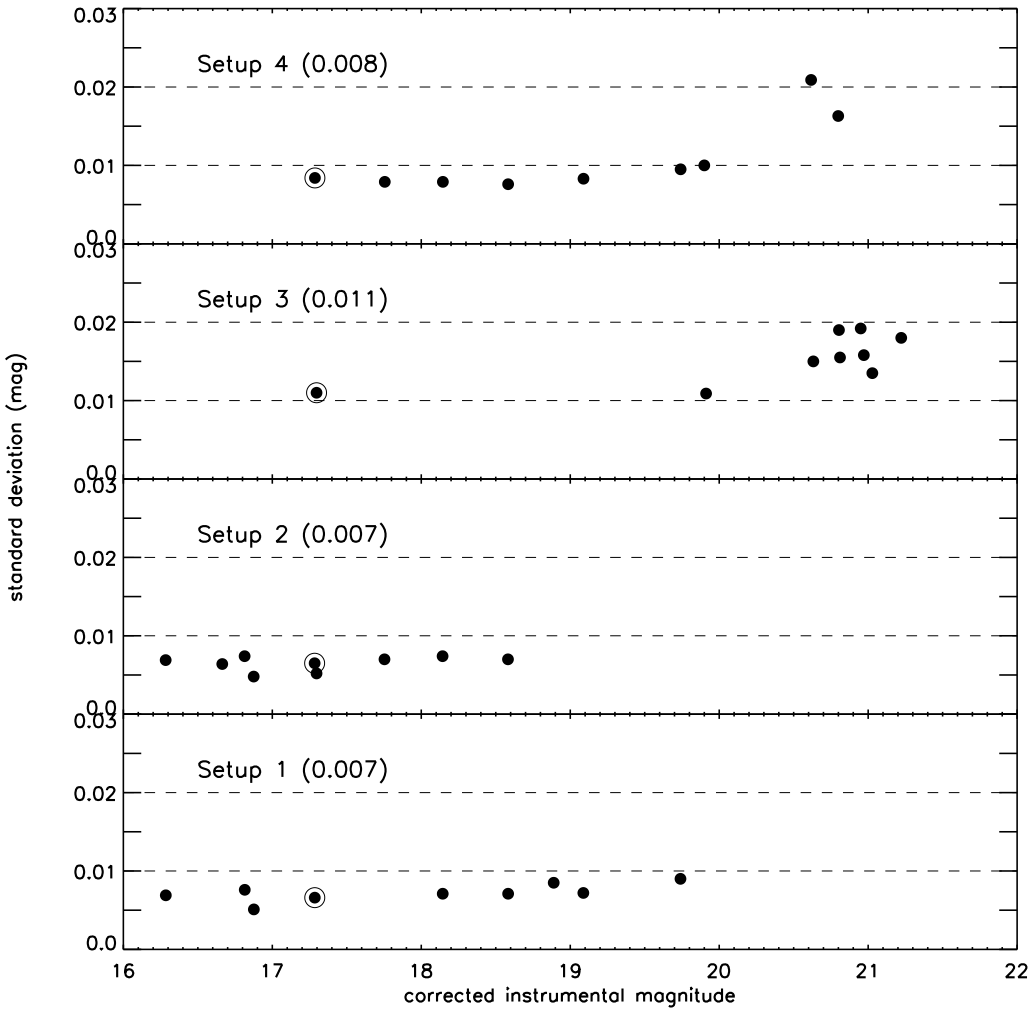

Fig. 4.— Standard deviations of LHS 3045 (given in the parenthesis) from different sets of reference stars in the field are shown. Points surrounded by open circles indicate LHS 3045 in each configuration. The details of different setups are discussed in §5.1.

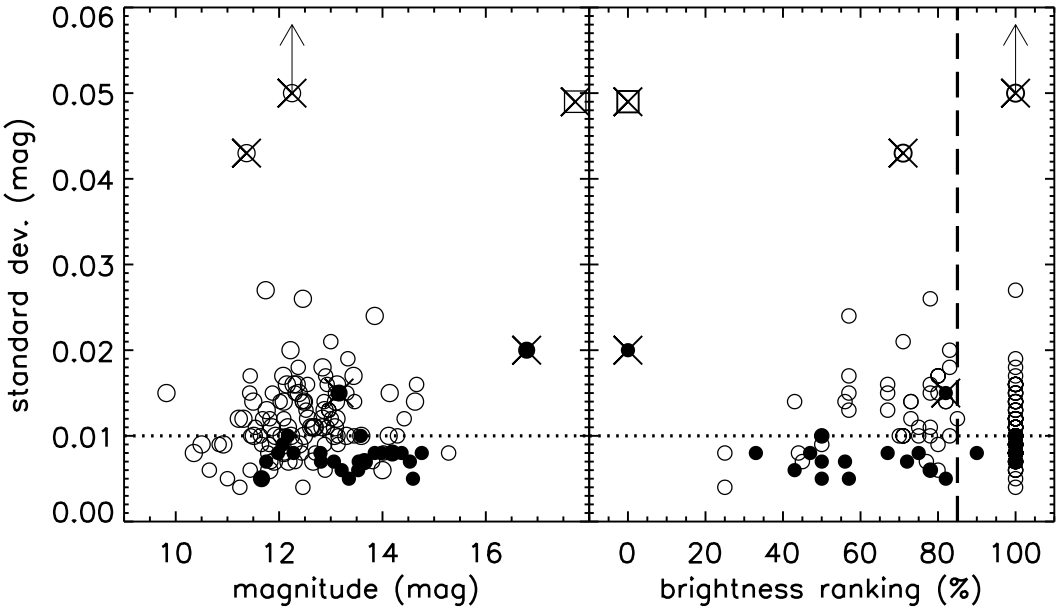

Fig. 5.— Variability measurements of 108 dwarfs (open circles) and 22 subdwarfs (solid circles) are plotted against their apparent magnitudes (left panel) and brightness rankings among all stars in each field (right panel). In the left panel, the apparent magnitudes correspond to V, R or I values, depending on the filter used for parallax observations. In the right panel, a vertical dashed line shows the mean brightness ranking of $\sim$85% for all 130 stars. Dotted lines mark a standard deviation value, σ_{mag}, of 0.010 mag. Five stars discussed in §5.1 are marked with Xs. The white dwarf, LHS 193B, is represented as an open box.

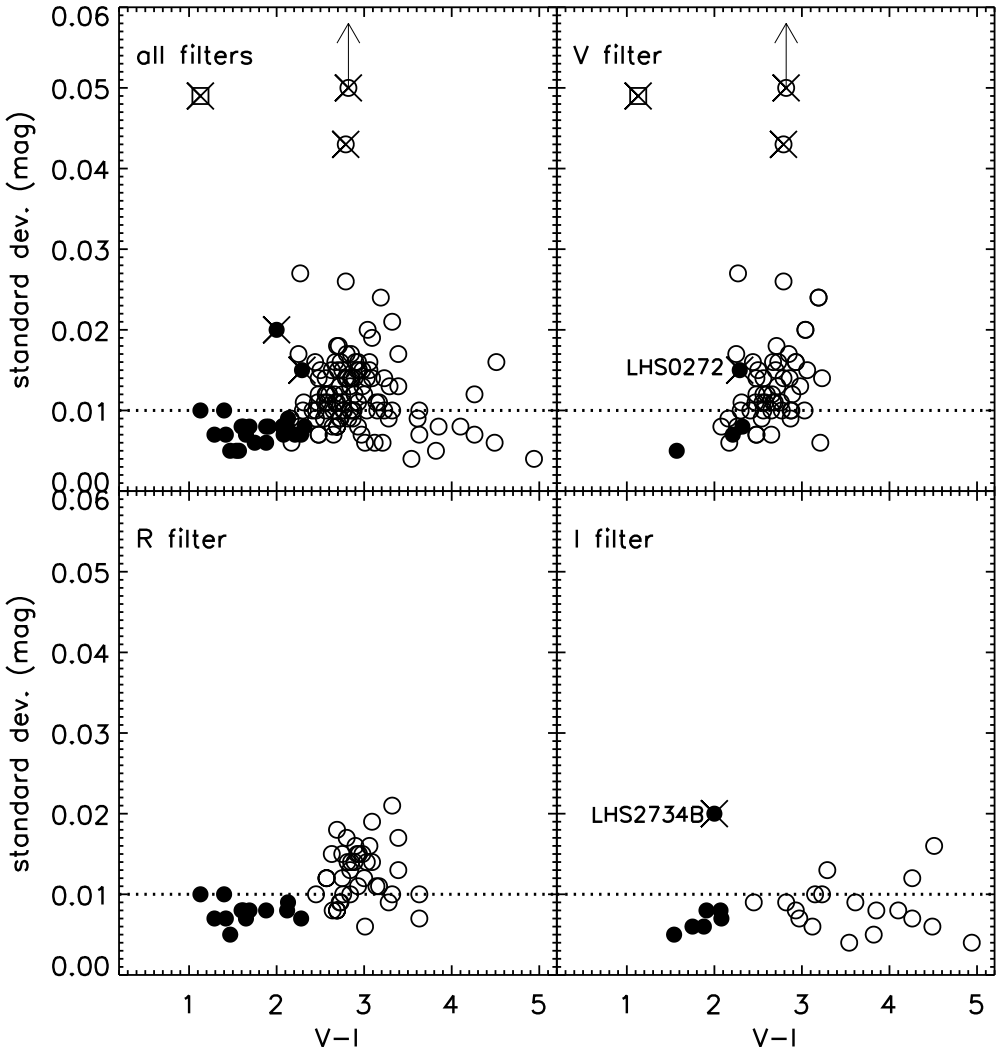

Fig. 6.— Variability measurements of 108 dwarfs (open circles) and 22 subdwarfs (solid circles) are plotted against their $(V - I)$ colors. The entire sample is shown in the upper left panel. Stars observed in V, R and I filters are plotted separately in the other three panels. LHS 272 and LHS 2734B are labeled and discussed in the text. Symbols have the same meanings as in Figure 5.

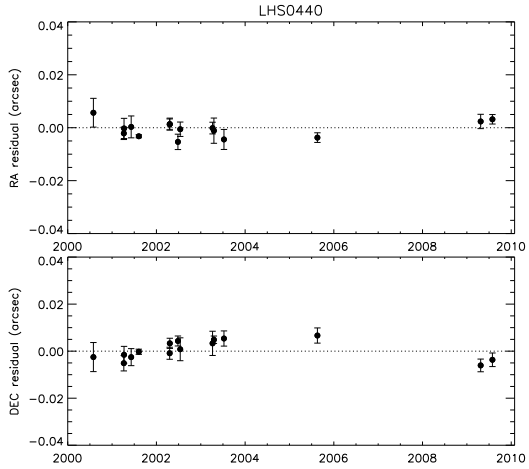

(a)

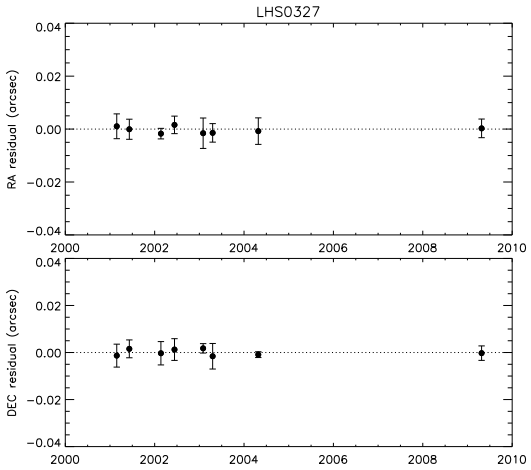

(b)

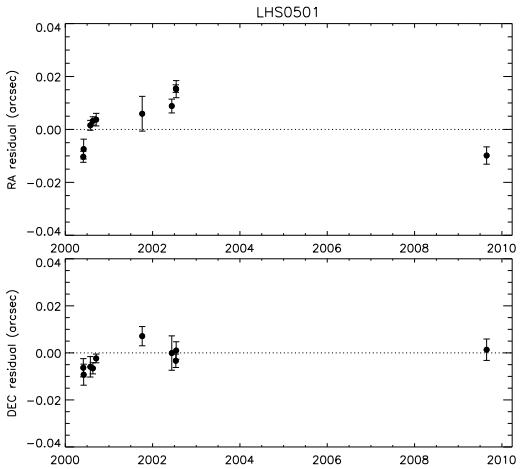

(c)

Fig. 7.— Nightly mean astrometric residuals in right ascension and declination are shown for LHS 440, LHS 327 (a typical star without a detected perturbation), and LHS 501. The astrometric signatures of each system's proper motion and parallax have been removed. [To Editor: Please arrange three plots horizontally from left (a) to right (c).]

Table 1.

Name	RA (J2000.0)	DEC	Filt	Nsea	Nfrm	Coverage	Years	Nref	π(rel) (mas)	π(corr) (mas)	π(abs) (mas)	μ (mas/yr)	P.A. (deg)	V_{tan} (km/s)	Note
(1)	(2)		(3)	(4)	(5)	(6)	(7)	(8)	(9)	(10)	(11)	(12)	(13)	(14)	
First Trigonometric Parallaxes															
G 266-089B	00 19 36.59	−28 09 38.8	V	5s	62	2000.87–2005.69	4.82	8	33.26±1.68	1.39±0.14	34.65±1.69	1370.8±0.9	192.1±0.07	187.5	!
G 266-089A	00 19 37.02	−28 09 45.7	V	5s	62	2000.87–2005.69	4.82	8	31.45±1.68	1.39±0.14	32.84±1.69	1372.2±0.9	192.3±0.07	198.1	!
LHS 124	00 49 29.05	−61 02 32.7	V	9s	57	2000.88–2008.87	7.99	7	47.44±1.38	1.18±0.14	48.62±1.39	1126.5±0.6	94.6±0.05	109.8	
LHS 125	00 50 17.09	−39 30 08.3	R	7s	48	2001.88–2008.86	6.98	5	11.90±3.49	2.06±0.16	13.96±3.49	1031.5±1.3	171.4±0.12	350.3	
LHS 164	03 01 40.58	−34 57 56.5	R	8s	83	2001.87–2009.03	7.16	7	18.19±1.55	0.97±0.11	19.16±1.55	1323.9±0.7	157.7±0.05	327.5	
LHS 176	03 35 38.61	−08 29 22.7	I	5s	47	2003.95–2009.12	5.17	7	76.35±1.30	1.42±0.08	77.77±1.30	1549.8±0.7	101.9±0.04	94.5	
SCR0342-6407	03 42 57.40	−64 07 56.5	I	4s	66	2003.94–2007.89	3.95	9	41.13±2.01	0.43±0.04	41.56±2.01	1059.9±0.9	143.3±0.10	120.9	
WT0135	04 11 27.14	−44 18 09.7	R	7s	59	2000.07–2009.78	9.71	5	38.38±2.42	0.66±0.04	39.04±2.42	691.5±0.8	67.1±0.13	84.0	
LSR0627+0616	06 27 33.33	+06 16 58.9	I	4c+	41	2002.95–2009.02	6.07	14	14.68±1.21	1.75±0.32	16.43±1.25	1009.0±0.9	179.0±0.07	291.1	!
LHS 272	09 43 46.16	−17 47 06.2	V	4s	61	2001.15–2005.06	3.91	10	72.81±1.17	1.14±0.11	73.95±1.18	1439.0±1.0	279.2±0.07	92.2	!
LHS 284	10 36 03.09	−14 42 29.1	I	3c	58	2003.08–2005.21	2.13	12	20.35±1.30	0.79±0.07	21.14±1.30	1085.6±1.3	297.8±0.13	243.4	
SCR1107-4135	11 07 55.90	−41 35 52.8	I	4s	55	2006.21–2009.25	3.04	8	13.82±1.18	0.97±0.08	14.79±1.18	1186.5±1.0	283.2±0.08	380.1	
LHS 323	12 17 30.16	−29 02 20.7	I	4s	46	2006.21–2009.23	3.02	8	22.46±1.83	0.83±0.04	23.29±1.83	1105.8±1.4	267.1±0.11	225.0	
LHS 327	12 25 50.73	−24 33 17.8	R	6s	50	2001.15–2009.31	8.16	9	9.98±1.40	0.84±0.11	10.72±1.40	981.6±0.6	262.6±0.05	433.8	!
GJ 1158	12 29 34.54	−55 59 37.1	V	6s+	76	2001.15–2008.21	7.06	10	73.60±1.15	2.58±0.77	76.18±1.38	1205.0±0.5	228.0±0.05	75.0	
LHS 347	13 10 01.80	+22 30 05.3	R	6s	54	2001.15–2009.32	8.17	5	15.73±2.29	0.99±0.09	16.72±2.29	1169.8±1.0	232.3±0.09	331.6	!
LHS 2734A	13 25 14.20	−21 27 12.4	I	3s	36	2003.09–2005.48	2.39	12	2.79±1.19	1.15±0.09	3.94±1.19	594.2±1.1	227.8±0.21	714.8	!
LHS 2734B	13 25 15.70	−21 28 18.0	I	3s	36	2003.09–2005.48	2.39	12	−1.70±1.52	1.15±0.09	3.94±1.19*	595.2±1.4	228.2±0.27	···	!
LHS 3045	15 14 54.39	−31 50 13.6	R	5s+	51	2006.21–2009.61	3.40	8	14.61±0.98	2.38±0.29	16.99±1.02	930.7±0.9	217.8±0.11	259.7	!
SIPS1529-2907	15 29 14.00	−29 07 37.7	I	4s	45	2006.22–2009.31	3.09	11	26.64±1.02	1.18±0.17	27.82±1.03	1016.9±0.9	187.7±0.08	187.7	
SCR1916-3638	19 16 46.57	−36 38 05.9	I	6s	56	2005.72–2009.49	3.77	8	12.51±1.19	2.27±0.68	14.78±1.37	1293.5±0.9	184.5±0.06	414.8	
LHS 3620	21 04 25.37	−27 52 46.8	I	6s	49	2003.52–2009.57	6.05	9	11.74±1.40	1.12±0.11	12.88±1.40	968.7±0.9	186.4±0.09	357.1	
SCR 2115-7541	21 15 15.09	−75 41 52.0	I	4s	75	2003.51–2006.57	3.06	12	30.88±1.26	2.05±0.22	32.96±1.28	1052.7±1.0	144.6±0.10	151.5	
LHS 3732	21 55 57.10	−45 39 34.3	R	4c	40	2005.70–2008.64	3.14	9	6.59±1.57	1.75±0.18	8.34±1.58	959.3±1.6	157.9±0.18	545.1	!
LHS 3740	21 58 53.18	−57 56 03.5	R	5s	52	2005.72–2009.78	4.06	5	34.74±1.45	1.20±0.10	35.94±1.45	908.9±1.0	95.7±0.09	121.8	
LHS 518	22 20 26.97	−24 21 49.5	R	5s+	84	2002.51–2009.54	7.03	11	15.41±1.31	0.51±0.09	15.92±1.31	1063.9±0.7	156.0±0.07	316.8	
Revised Parallaxes															
LHS 193B	04 32 35.98	−39 02 14.6	V	6s	78	2000.87–2009.74	8.87	8	30.77±2.40	2.21±0.21	32.98±2.41	999.2±1.2	44.7±0.14	143.6	
LHS 193A	04 32 36.56	−39 02 03.4	V	6s	78	2000.87–2009.74	8.87	8	32.55±1.43	2.21±0.21	34.76±1.45	993.8±0.6	44.7±0.07	135.5	1
LHS 205	05 16 59.67	−78 17 20.2	V	7s	64	2003.95–2009.75	5.80	6	64.48±1.89	0.87±0.24	65.35±1.91	1134.1±1.2	179.0±0.09	82.3	2
GJ 1129	09 44 47.34	−18 12 48.9	V	5s	48	2000.06–2004.33	4.27	7	92.38±2.48	1.51±0.30	93.89±2.49	1597.3±1.3	264.3±0.07	80.6	3
LHS 300AB	11 11 13.68	−41 05 32.7	R	6s	76	2001.15–2009.31	8.16	11	31.38±1.35	1.65±0.17	33.03±1.36	1251.5±0.6	263.9±0.04	179.6	4
LHS 318	11 56 54.87	+26 39 56.3	I	5s	57	2003.25–2009.25	6.00	6	18.10±2.32	0.66±0.05	18.76±2.32	1360.3±1.4	154.5±0.11	343.7	5, !
LHS 326	12 24 26.81	−04 43 36.7	R	4s	66	2003.09–2008.38	5.29	7	19.59±1.94	0.80±0.07	20.39±1.94	1301.3±0.7	241.8±0.06	302.4	6, !
LHS 406	15 43 18.33	−20 15 32.9	R	6s	81	2000.57–2009.31	8.74	12	44.98±1.14	1.75±0.28	46.73±1.17	1160.8±0.5	194.8±0.04	117.7	7
LHS 440	17 18 25.58	−43 26 37.6	R	6s	100	2000.58–2009.58	9.00	10	34.52±1.09	1.88±0.54	36.40±1.22	1082.5±0.5	233.3±0.05	141.0	8, !
LHS 475	19 20 54.26	−82 33 16.1	V	9s	132	2000.57–2009.54	8.97	8	81.68±0.93	1.36±0.08	83.04±0.93	1269.6±0.3	164.5±0.02	72.5	9
LHS 499	20 51 41.64	−79 18 39.9	V	4s	63	2004.56–2007.75	3.19	7	55.51±2.11	1.42±0.17	56.93±2.12	1209.2±1.7	143.9±0.16	100.7	10, !
LHS 500	20 55 37.12	−14 03 54.8	V	5s	71	1999.70–2009.73	10.03	9	81.91±1.24	0.88±0.05	82.79±1.24	1490.8±0.5	108.3±0.03	85.4	11, !
LHS 501	20 55 37.76	−14 02 08.1	V	5s	71	1999.70–2009.73	10.03	9	72.20±1.17	0.88±0.05	73.08±1.17	1297.6±0.4	108.2±0.03	84.2	12, !
LHS 521	22 27 59.21	−30 09 32.8	R	5c	76	2000.58–2009.54	8.96	8	17.24±1.07	1.22±0.09	18.46±1.07	1006.8±0.6	137.2±0.07	258.5	13, !
GJ 1277	22 56 24.66	−60 03 49.2	V	8s+	80	2001.87–2007.82	5.95	7	96.31±0.95	1.17±0.69	97.48±1.17	1082.0±0.6	210.4±0.06	52.6	14, !

Note. — N_{sea} indicates the number of seasons observed, where 2–3 months of observations count as one season, for seasons having more than 3 images taken. The letter "c" indicates a continuous set of observations where multiple nights of data were taken in each season, whereas an "s" indicates scattered observations when one or more seasons have only a single night of observations. Generally, "c" observations are better. A + indicates that three or fewer individual images are used in one or more seasons

that are not counted in N_{sea}. Stars with exclamation marks in the Notes column are discussed in Section 6. The * indicates that the absolute parallax of LHS 2734B has been adopted from LHS 2734A. All previous parallax measurements listed here are absolute parallaxes, other than GJ1277, which is a relative parallax: (1) Parallax of 32.06±1.65 mas in Jao et al. (2005). (2) Parallax of 77.50±11 mas in YPC. (3) Parallax of 90.93±3.78 mas in Jao et al. (2005). (4) Parallax of 32.30±1.85 mas in Jao et al. (2005). (5) Parallax of 24.8±6 mas in Smart et al. (2007). (6) Parallax of 11.7±4.3 mas in Smart et al. (2007). (7) Parallax of 47.28±1.61 mas in Jao et al. (2005). (8) Parallax of 36.90±2.19 mas in Jao et al. (2005). (9) Parallax of 78.34±2.03 mas in Jao et al. (2005). (10) Parallax of 63.0±11.7 mas in YPC. (11) Parallax of 81.95±1.54 mas in Jao et al. (2005). (12) Parallax of 77.59±1.49 mas in Jao et al. (2005). (13) Parallax of 21.60±1.59 mas in Jao et al. (2005). (14) Relative Parallax of 94±1.0 mas in Bartlett et al. (2009).

Table 2.

Name1	Name2	V mag	R mag	I mag	#	π filter	σ mag	No. of Nights	J mag	H mag	K_s mag	Spect.	Refs
(1)	(2)	(3)	(4)	(5)	(6)	(7)	(8)	(9)	(10)	(11)	(12)	(13)	(14)
G 266-089B	LHS 110	14.19	13.17	11.87	2	V	0.008	13	10.63±0.02	10.12±0.03	9.88±0.02	M4.0J[VI]	1
G 266-089A	LHS 111	13.65	12.66	11.44	2	V	0.007	13	10.25±0.02	9.73±0.03	9.48±0.02	M4.0J[VI]	1
LHS 124	GJ 1022	12.17	11.12	9.86	2	V	0.011	15	8.63±0.02	8.09±0.05	7.84±0.03	M2.0V	1
LHS 125	LP 989-183	14.32	13.58	12.92	2	R	0.010	10	12.05±0.02	11.58±0.02	11.45±0.03	K4.0[VI]	6
LHS 164	LEHPM 2991	13.56	12.81	12.14	3	R	0.007	18	11.38±0.03	10.77±0.02	10.64±0.02	K7.0VI	6
LHS 176	NLTT 11328	15.92	14.30	12.31	3	I	0.009	11	10.38±0.02	9.80±0.02	9.46±0.02	M5.0V	1
SCR 0342-6407		16.01	14.65	12.89	2	I	0.006	13	11.32±0.02	10.87±0.03	10.58±0.02	M4.0V	1
WT0135	LEHPM 3673	14.10	13.06	11.82	2	R	0.007	12	10.55±0.02	10.12±0.03	9.83±0.02	M3.0VI	6
LSR 0627+0616		16.28	15.31	14.37	2	I	0.008	10	13.29±0.03	12.83±0.03	12.63±0.03	esdM1.5	7
LHS 272	NLTT 22460	13.16	12.10	10.87	3	V	0.015	13	9.62±0.02	9.12±0.02	8.87±0.02	M3.0VI	6
LHS 284	NLTT 24803	16.78	15.49	13.81	3	I	0.007	13	12.28±0.02	11.79±0.03	11.58±0.03	M4.0V	1
SCR1107-4135		14.96	14.07	13.21	2	I	0.006	12	12.19±0.02	11.69±0.02	11.47±0.02	M0.5VI	6
LHS 323	NLTT 30238	16.95	15.66	14.02	2	I	0.008	9	12.54±0.02	12.05±0.02	11.78±0.02	M4.0V	1
LHS 327	NLTT 30709	12.75	12.17	11.62	2	R	0.010	10	10.81±0.02	10.31±0.02	10.14±0.02	K4.0[VI]	6
GJ1158	LHS 322	13.26	12.02	10.41	3	V	0.014	16	8.89±0.03	8.35±0.04	8.07±0.02	M3.0V	2
LHS 347	NLTT 33109	12.42	11.75	11.13	2	R	0.007	11	10.26±0.02	9.71±0.03	9.59±0.02	K2.0[VI]	1
LHS 2734A	LP 797-61	16.13	15.32	14.59	2	I	0.005	7	13.63±0.03	13.10±0.03	12.90±0.04	K7.0VI	6
LHS 2734B		18.79	17.93	16.79	2	I	0.020	7	15.83±0.09	15.30±0.09	14.93±0.14	M1.0VI:	6
LHS 3045	NLTT 39664	14.39	13.54	12.74	2	R	0.007	13	11.76±0.02	11.23±0.03	11.00±0.02	[VI]	1
SIPS 1529-2907		19.38	17.52	15.28	4	I	0.008	11	13.32±0.03	12.86±0.02	12.50±0.02	M6.5V	1
SCR 1916-3638		16.83	15.82	14.76	3	I	0.008	13	13.66±0.02	13.12±0.02	12.95±0.03	M3.0VI	6
LHS 3620	NLTT 50449	16.61	15.59	14.53	2	I	0.007	13	13.41±0.02	12.89±0.02	12.70±0.03	M2.0VI	6
SCR 2115-7541		14.48	13.25	11.66	3	I	0.009	15	10.14±0.02	9.60±0.02	9.33±0.02	M3.5V	1
LHS 3732	L 355-29	14.11	13.35	12.64	3	R	0.005	9	11.72±0.02	11.14±0.02	11.00±0.02	VI	4
LHS 3740	L 213-75	14.06	12.88	11.33	2	R	0.009	13	9.85±0.02	9.27±0.02	9.00±0.02	M3.5V	1
LHS 518	NLTT 53550	13.63	12.80	12.01	2	R	0.008	18	11.04±0.02	10.59±0.02	10.39±0.02	M1.0VI	6
LHS 193B		17.73	17.18	16.60	3	V	0.049	13	16.21± ···	15.94± ···	··· ± ···	WD	5
LHS 193A	L 447-10	11.66	10.85	10.09	3	V	0.005	13	9.18±0.02	8.55±0.02	8.43±0.02	K6.0VI	6
LHS 205	GJ 1077	11.90	10.81	9.42	4	V	0.007	14	8.07±0.02	7.44±0.02	7.20±0.02	M2.0V	2
GJ 1129	LHS 273	12.46	11.24	9.67	3	V	0.026	10	8.12±0.03	7.54±0.04	7.26±0.02	M3.5V	3
LHS 300A	L 395-13	13.18	12.28	11.49	2	R	0.008	13	10.48±0.02	10.01±0.03	9.80±0.02	M0.0VI:	6
LHS 318	NLTT 29045	15.41	14.48	13.53	3	I	0.006	14	12.50±0.02	11.98±0.02	11.80±0.02	M2.0VI:	6
LHS 326	NLTT 30636	14.92	13.98	13.04	2	R	0.008	14	11.93±0.02	11.43±0.02	11.23±0.02	M3.0VI	6
LHS 406	NLTT 40994	13.06	12.07	10.93	2	R	0.009	17	9.78±0.02	9.23±0.02	9.02±0.02	M2.0VI	6
LHS 440	L 413-156	12.98	11.98	10.86	2	R	0.008	17	9.70±0.02	9.13±0.02	8.95±0.02	M1.0VI:	6
LHS 475	L 22-69	12.69	11.51	10.00	4	V	0.011	26	8.56±0.03	8.00±0.04	7.69±0.04	M3.0V	2
LHS 499	GJ 808	11.81	10.82	9.64	2	V	0.006	12	8.46±0.03	7.91±0.05	7.66±0.02	M1.5V	2
LHS 500	GJ 810B	14.63	13.21	11.40	2	V	0.014	14	9.72±0.02	9.22±0.02	8.92±0.02	M5.0V	2
LHS 501	GJ 810A	12.48	11.23	9.62	2	V	0.014	14	8.12±0.03	7.64±0.04	7.37±0.03	M4.0V	2
LHS 521	LP 932-1	14.70	13.85	13.10	2	R	0.008	16	12.13±0.02	11.66±0.03	11.46±0.02	M0.5VI:	6
GJ1277	LHS 532	14.00	12.59	10.79	3	V	0.006	20	8.98±0.03	8.36±0.03	8.11±0.02	M4.5V	1

Note. — Brackets [ ] indicate a possible luminosity class. A colon : indicates a questionable subtype.

References. — (1) this work; (2) Hawley et al. 1996; (3) Henry et al. 2002; (4) Ibata & Irwin 1997; (5) Jao et al. 2005; (6) Jao et al. 2008; (7) Lépine et al. 2003

Name	Old V		New V		Combined
	σ_{mag}	Nfrm	σ_{mag}	Nfrm	σ_{mag}
LHS 145	0.007	115	0.005	50	0.007
GJ 440	0.008	124	0.006	50	0.007
GJ 781.3	0.007	86	0.006	48	0.007

Table 3: Variability comparisons of three white dwarfs using the old and new V filters. The σ_{mag} values represent the standard deviations of the photometry calculated via the method described in the text. The "Nfrm" values correspond to the total number of frames used in each filter. The combined variabilities are from Subasavage et al. (2009) and have been measured using the same methodology.